PROTEINS: Structure, Function, and Bioinformatics 55:835–845 (2004)

Solution Structure of BmKK2, a New Potassium Channel Blocker from the Venom of Chinese Scorpion *Buthus martensi* Karsch

Naixia Zhang,[1] Minghua Li,[2] Xiang Chen,[1] Yuefeng Wang,[1] Gong Wu,[1] Guoyuan Hu,[2] Houming Wu[1]*

[1]*State Key Laboratory of Bio-organic and Natural Products Chemistry, Shanghai Institute of Organic Chemistry, Chinese Academy of Sciences, Shanghai, People's Republic of China*

[2]*State Key Laboratory of Drug Research, Shanghai Institute of Materia Medica, Shanghai Institutes for Biological Sciences, Chinese Academy of Sciences, Shanghai, People's Republic of China*

ABSTRACT **A natural K^+ channel blocker, BmKK2 (a member of scorpion toxin subfamily α-KTx 14), which is composed of 31 amino acid residues and purified from the venom of the Chinese scorpion *Buthus martensi* Karsch, was characterized using whole-cell patch-clamp recording in rat hippocampal neurons. The three dimensional structure of BmKK2 was determined with two-dimensional NMR spectroscopy and molecular modelling techniques. In solution this toxin adopted a common α/β-motif, but showed distinct local conformation in the loop between α-helix and β-sheet in comparison with typical short-chain scorpion toxins (e.g., CTX and NTX). Also, the α helix is shorter and the β-sheet element is smaller (each strand consisted only two residues). The unusual structural feature of BmKK2 was attributed to the shorter loop between the α-helix and β-sheet and the presence of two consecutive Pro residues at position 21 and 22 in the loop. Moreover, two models of BmKK2/hKv1.3 channel and BmKK2/rSK2 channel complexes were simulated with docking calculations. The results demonstrated the existence of a α-mode binding between the toxin and the channels. The model of BmKK2/rSK2 channel complex exhibited favorable contacts both in electrostatic and hydrophobic, including a network of five hydrogen bonds and bigger interface containing seven pairs of inter-residue interactions. In contrast, the model of BmKK2/hKv1.3 channel complex, containing only three pairs of inter-residue interactions, exhibited poor contacts and smaller interface. The results well explained its lower activity towards Kv channel, and predicted that it may prefer a type of SK channel with a narrower entryway as its specific receptor. Proteins 2004;55:835–845.** © 2004 Wiley-Liss, Inc.

Key words: BmKK2; *Buthus martensi* Karsch; scorpion toxin; NMR solution structure; potassium channel blocker; rSK channel; Kv channel

INTRODUCTION

Ion channels play crucial roles in regulating a variety of cellular processes in both excitable and non-excitable cells. Scorpion peptides, which bind to various ion channels with high affinity and specificity, widely serve as useful tools in probing the protein mapping of ion channels and clarifying the molecular mechanism involved in channel gating and signal transduction. These peptides have been classified into two major groups according to their primary structures and biological function: (1) group I mainly acts on sodium channels and covers peptides of 60–70 amino acids linked by four disulfide bridges;[1–3] (2) group II interacts specifically with potassium or chloride channels and contains peptides of 20–40 amino acids linked by three or four disulfide bridges.[4–8]

Scorpion peptides blocking potassium channels have provided the first indirect information concerning K^+ channel structure.[9] In addition, these peptides became invaluable tools for purification K^+ channel proteins from native tissues,[10] and also for understanding the physiological role of a specific K^+ channel.[11] The first K^+ channel-blocking peptide found in scorpion venom was noxiustoxin (NTX).[12] Since then, a variety of of K^+ channel-blocking toxins were isolated as native peptides from scorpion venoms, and a number of toxins were identified from their cDNA sequences. All known K^+ channel toxins, found in scorpion venoms thus far have been divided into 17 subfamilies mainly according to their primary structures (amino acid or cDNA sequences).[13, 14] These K^+ channel specific toxins interact on three major classes of potassium channels: voltage-gated (Kv-type), high-conductance Ca^{2+}-activated (BK-type) and small-conductance Ca^{2+}-acti-

Abbreviations: 1D, one-dimensional; 3D, three-dimensional; NMR, nuclear magnetic resonance; DQF-COSY, double-quantum-filtered shift correlated spectroscopy; Kv channel, voltage-gated potassium channel; NOESY, nuclear Overhauser enhancement spectroscopy; RMSD, root-mean-square deviation; rSK channel, rat small-conductance calcium-activated potassium channel; TOCSY, total correlation spectroscopy

Grant sponsor: the National Science Foundation of China; Grant number: 20132030; Grant sponsor: Chinese Academy of Sciences; Grant sponsor: State Minister of Science and Technology of China.

*Correspondence to: Houming Wu, Shanghai Institute of Organic Chemistry, Chinese Academy of Sciences, Shanghai, 200032, P.R. China. E-mail: hmwu@mail.sioc.ac.cn

Received 20 October 2003; Accepted 24 December 2003

Published online 1 April 2004 in Wiley InterScience (www.interscience.wiley.com). DOI: 10.1002/prot.20117

vated (SK-type). The three-dimensional structures of several K^+ channel toxins in scorpion venoms, such as CTX,[15] NTX,[16] BmTX1/2,[17] P05-NH2,[18] KTX,[19] Tc1,[20] BmP01/03[21, 22] etc., have been determined by NMR spectroscopy. Although a common global folding of α/ β scaffold was found in the solution structures of these peptides, there are subtle variations among them in amino acid sequence, the size of β-sheet, the type of β-turn, or the type and the size of α-helix. These structural variations may contribute to their distinct selectivity and affinity towards different K^+ channels.

In this manuscript, we report electrophysiological characterization, and the 3D solution structure of a new K^+ channel toxin BmKK2 isolated from the venom of Chinese scorpion *Buthus martensi* Karsch. The cDNA sequence KK2, which encodes BmKK2 peptide, has been cloned from the gland of *Buthus martensi* Karsch by Zeng et al.[23] and the peptide BmKK2 has been classified as a member of the scorpion K^+ channel toxin subfamily α-KTx 14.[14] To date, no three-dimensional structure of K^+ channel toxin in this subfamily has been reported. The solution structure of BmKK2 described here reveals some unusual features of this molecule, and the results derived from the docking experiments predict some basic characteristics for the K^+ channel that binds specifically with the toxin.

MATERIALS AND METHODS

Electro-Physiological Characterization of BmKK2

Dissociated neurons were prepared as described previously.[24] Briefly, mini-slices (500 üm) of hippocampal CA1 region of 5–9-day-old Sprague-Dawley rats were cut in oxygenated ice-cold dissociation solution containing (in mM): Na_2SO_4 82, K_2SO_4 30, $MgCl_2$ 5, N-(2-hydroxyethyl) piperazine-N′-(2-ethanesulfonic acid) (HEPES) 10 and glucose 10 at pH 7.3 with NaOH. The slices were incubated in dissociation solution containing 3mg/ml protease XXIII at 32°C for 8 min, then placed in dissociation solution containing 1 mg/ml trypsin inhibitor type II-S and 1 mg/ml bovine serum albumin at room temperature under an oxygen atmosphere. Before recording the slices were triturated using a series of fire-polished Pasteur pipettes with decreasing tip diameters. Dissociated neurons were placed in recording dish and perfused with external solution containing (in mM): NaCl 135, KCl 5, $MgCl_2$ 2, $CaCl_2$ 1, HEPES 10, glucose 10 and tetrodotoxin 0.001 at pH 7.3 with NaOH.

Whole-cell voltage-clamp recording was made from large pyramidal-shaped neurons using an Axopatch 200A amplifier at 21–23°C. The electrodes (tip resistance 2–4 MΩ) were filled with pipette solution containing (in mM): potassium gluconate 125, KCl 20, $MgCl_2$ 2, $CaCl_2$ 1, HEPES 10, EGTA 10. The holding potential was −50 mV. Voltage protocols were provided by pClamp 6.2 software via a DigiData-1200A interface. The total $\underline{K^+}$ currents were elicited by depolarizing command pulses to +60 mV in 10 mV steps following a hyperpolarizing prepulse of 400 ms to −110 mV. The delayed rectifier K^+ currents (I_K) were elicited by a similar protocol in which a 50 ms interval at −50 mV was inserted after the prepulse. Subtraction of I_K from the total K^+ currents revealed the fast transient K^+ current (I_A).[25] Current records were filtered at 2–10 KHz and sampled at frequencies of 10−40 KHz. Series resistance was compensated by 75–80%. Linear leak and residual capacitance currents were subtracted on-line. Sample of BmKK2 was dissolved in external solution and the toxin-containing solution was directly applied to the recorded neuron using RSC-100 Rapid Solution Changer. The data are presented as mean ±S.E.M.

NMR Experiments

The BmKK2 used was isolated from the venom of the Chinese scorpion *Buthus martensi* Karsch as described previously.[26] The peptide BmKK2 was dissolved in H_2O/D_2O (90/10 v/v) or 100% D_2O, pH 3.0 or pH 2.6, uncorrected for isotope effects, adjusted by adding micro-liter of dilute DCl or NaOD. The final concentration of BmKK2 was about 2.7 mmol/L. The amide proton exchange rate was determined after lyophilization and re-dissolution in 100% D_2O.

All the NMR experiments were recorded on a Varian unity Inova 600 spectrometer at 300 K. To solve assignment ambiguities the experiments were performed at two pH values of 3.0 and 2.6. Quadrature detection was employed in all experiments and the carrier frequency always maintained at the solvent resonance. Presaturation was used to suppress the water peak in all experiments. Two-dimensional double-quantum-filtered correlation spectroscopy (DQF-COSY),[27] total correlation spectroscopy (TOCSY),[28,29] and nuclear Overhauser enhancement spectroscopy (NOESY)[30] were recorded in phase-sensitive mode by using the time-proportional phase incrementation method.[31] All the two-dimensional spectra were measured with 4K data points in t_2 dimension and 512 data points in t_1 dimension. The TOCSY spectra were recorded using the MELV-17 pulse sequence with mixing times of 80 and 120 ms,[32] and the NOESY spectra were acquired using mixing times of 200 and 300 ms. For determination of slowly exchanging protons at pH 3.0, a series of 1D spectra during the first 3 hours followed by three TOCSY spectra (τ_m = 80 ms, 8 h) were recorded at 300 K immediately after the sample was dissolved in D_2O. A Shifted sine window function and zero-filling was applied prior to Fourier transformation. The experimental data were acquired and processed using Vnmr 6.1B program. The processed data were analyzed with XEASY[33] for visualization of NMR spectra, peak-picking and peak-integration on a SGI Indigo II R 5000 computer.

Assignment Strategy and Structure Calculation

The identification of amino acid spin systems and the sequential assignment were done using the standard strategy described by Wüthrich.[34]

The NOESY (200 ms) spectrum was used to generate the distance constraints. Dihedral angle constraints were derived from $^3J_{HNH\alpha}$ coupling constants, which were obtained by analyses of absorptive and dispersive rows of the DQF-COSY spectrum. Additional constraints were used to enforce hydrogen bonds implicated by the H-D exchange

TOCSY spectra. Distance geometry calculations were performed with the target function program DYANA[35] on a SGI Indigo II station. The 35 structures with the lowest constraint violations were subjected to restrained energy minimization (REM) performed with the AMBER 5.0 package.[36,37] Fifteen (15) best conformers with the lowest energy were used to represent the solution conformation of BmKK2. The programs PROCHECK and PROCHECK_NMR were used to analyze the NMR structures of BmKK2.[38,39] In addition, for visual comparison of the structures, 3D conformations were produced with the molecular graphics program MOLMOL[40] on a SGI indigo II computer. For pair of conformers, superposition and RMSD values for various subsets of atoms were calculated. The mean solution conformation was obtained by superimposing the 15 lowest energy AMBER conformers and then averaging the Cartesian coordinates of the corresponding atoms in the 15 superimposed conformers.

Docking of BmKK2 on a Model of hKv1.3 and a Model of rSK2

The complex models of hKv1.3 and rSK2 channels[41,42] were generated by the homology modeling on the basis of the crystal structure of the bacterial KcsA channel[43] using software SYBYL6.3 (Tripos Associates, 1996). The sequence alignment between KcsA and the other two potassium channels was obtained using the same criteria as those described by Gao et al.[44] The homology models of hKv1.3 and rSK2 were further subjected to Powell minimization (2000 steps) using Kollman force field. The RMSD for the structure of hKv1.3 and rSK2 are 0.82 Å and 0.90 Å, respectively, compared to the structure of KcsA.

The program O (version 8.0.6) was used for the docking experiment.[45] BmKK2 was docked manually into the outer of entryway of the hKv1.3 and rSK2 channel models along with the dipole direction. As expected, the mouth of the rSK2 K^+ channel bears a large negative charge, whereas the surface of BmKK2 toxin has a positive charge. The electrostatic potential between the BmKK2 toxin and K^+ channels attracted the positively-charged toxin to the entryway of the channel. In order to obtain favorable toxin-channel clusters, the toxin molecule was allowed to rotate during the docking process. The most stable cluster with the best fitting between toxin and K^+ channels was used to analyze the contacts between BmKK2 toxin and the K^+ channel.

The peptide/K^+ channel clusters docked most favorably were further subjected to energy minimization for 2000 steps to achieve the gradient tolerance 0.05 kcal/(mol Å) using the Powell algorithm and the Kollman force field in the software SYBYL6.3. Molecular dynamics simulation using the Powell algorithm was then carried out for these complexes for 100 fs at 300 K. Kollman force field constraints were applied on the backbones of the regions comprising residues Phe360 to Phe383 in Kv1.3 and residues Ala327 to Met350 in rSK2 channel, respectively, while the remaining part of the channel was kept fixed during the simulation. The structures of the peptides were completely unconstrained. A cutoff distance of 8 Å was used for non-bounded interactions. An integration timestep of 0.1 fs was used and coordinate sets of the trajectory were saved every 2 fs. Every structure obtained from the coordinate sets over the 100 fs of simulation was performed with 500 steps of minimization. Finally, the average structure was energy minimized with 1000 steps of Powell minimization.

RESULTS AND DISCUSSION

Electrophysiology Activity

Electro-physiological studies of the action of BmKK2 on voltage-gated K^+ channel (Kv channel) were performed, using conventional patch-clamp recording methods on dissociated rat hippocampal neurons. Scorpion toxin BmKK2 selectively inhibited the delayed rectifying potassium current (I_K). With the voltage protocols and subtraction procedure used, two types of outward current could be simultaneously obtained from the same neuron in the presence of 1 μM tetrodotoxin. The slowly inactivating outward current was reversibly blocked by 20 mM TEA, thus corresponded to the delayed rectifying potassium current I_K as shown in Figure 1(a) and 1(b). In Figure 1(c) current-voltage (I/V) relationships relative to peak K^+ currents are shown for control conditions and perfusion in the presence of toxin. The rapidly inactivating outward current was reversibly blocked by 10 mM 4-AP, and represented the fast transient potassium current I_A [Fig. 1(d and e)]. The current-voltage relationship curves [Fig. 1(f)] indicate that the toxin did not inhibit current I_A. Application of 1–300 μM scorpion toxin BmKK2 selectively inhibited I_K, leaving I_A unaffected. The inhibition was reversible upon washout. The inhibition was concentration-dependent: 30 and 100 μM scorpion toxin BmKK2 inhibited I_K to 79 ± 0.4% and 65 ± 2% of its control level, respectively.

NMR Resonance Assignment

The sequence-specific resonance assignment of BmKK2 was achieved according to the general procedure developed by Wüthrich.[34] The spin systems were identified on the basis of the DQF-COSY and the TOCSY spectra. The fingerprint region of the DQF-COSY spectra recorded in H_2O showed most of the H_N/H_α cross peaks expected and then the TOCSY spectra were used to correlate the side-chain spin-systems to the H_α and H_N protons for each residue. Intra-residue NOESY cross-peaks were used to discriminate Asp/Asn residues.

The spin systems were connected in sequence by virtue of $d_{\alpha N}(i, i+1)$, $d_{NN}(i, i+1)$ and $d_{\beta N}(i, i+1)$ NOE correlations in well-dispersed NOESY spectra. For BmKK2, the unique residues, Ile5 and Ser14, were used as the first starting positions for defining the sequential assignment. Starting from these two amino acids, the sequential assignment of segment 1–21 was obtained via $d_{\alpha N}(i, i+1)$, $d_{NN}(i, i+1)$ and $d_{\beta N}(i, i+1)$ NOE cross peaks. In this segment three proline residues were connected to their vicinal residues by $d_{\alpha\delta}(i, i+1)$, and $d_{N\delta}(i, i+1)$ correlation peaks. The remaining proline, phenylalanine and alanine residues, which were assigned as Pro22, Phe27 and Ala29 were then used as the

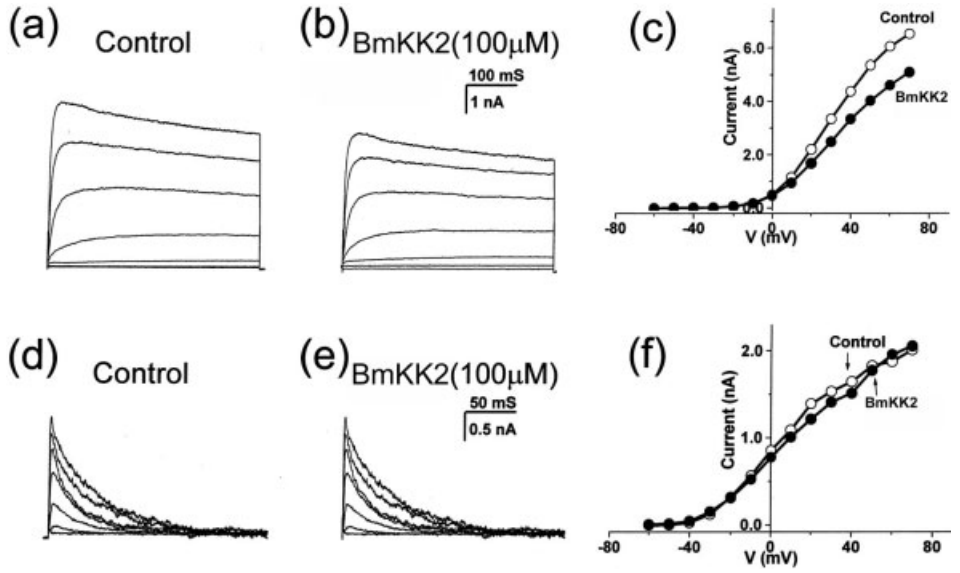

Fig. 1. Scorpion toxin BmKK2 selectively inhibits the delayed rectifying potassium current in hippocampal CA1 pyramidal neurons. **a, b**: The delayed rectifying potassium currents (I_K) evoked by depolarizing command pulses before and during application of scorpion toxin BmKK2. **d, e**: The fast transient potassium currents (I_A) evoked by depolarizing command pulses before and during application of the toxin. **c**: The current-voltage (I/V) relationship of I_K from the same neuron as shown in (a, b) before and during application of the toxin. **f**: The current-voltage (I/V) relationship of I_A from the same neuron as shown in (d, e) before and during application of the toxin.

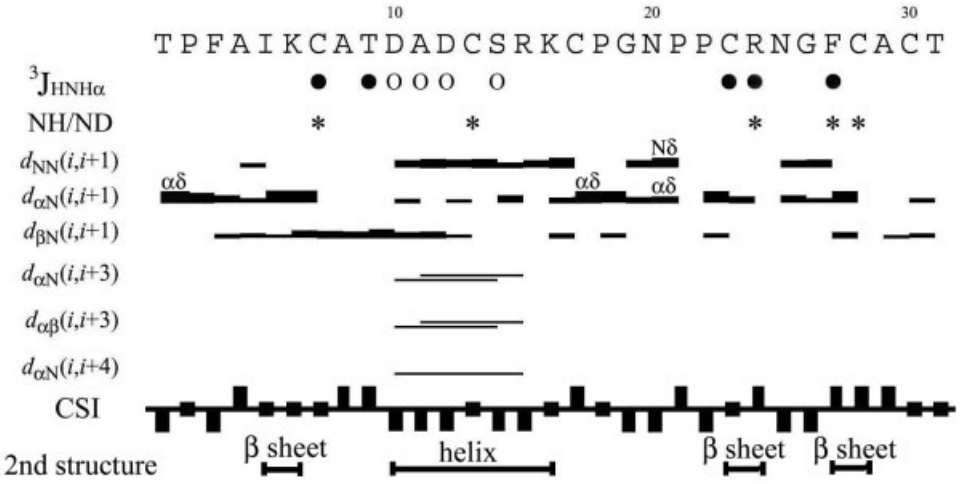

Fig. 2. Summary of NOE connectivities, J-coupling constant $^3J_{HNH\alpha}$, the amide proton exchange rate, and C$^\alpha$H chemical shift index. The thickness of the bar indicates the intensity of NOEs. Asterisks represent the NH protons in slowly exchanging. J-coupling constant $^3J_{HNH\alpha}$ are smaller than 6.0 Hz (open circle) and bigger than 8 Hz (filled circle). Positive bars and negative bars in the chemical shift index indicate the C$^\alpha$H protons downfield-shifted and up-field-shifted by $>$ 0.1 ppm, respectively as compared with the C$^\alpha$H proton chemical shifts of random-coil.

starting points for the sequential assignments of the C-terminal segments 22–24, 25–28 and 29–31, respectively. The sequence-specific assignments of these three segments were achieved by using the $d_{\alpha N}$(i, i+1) or the $d_{\beta N}$(i, i+1) correlation peaks. The sequential connectivities are illustrated in Figure 2. In addition, the medium-range NOE contacts such as $d_{\alpha N}$(i, i+3), $d_{\alpha N}$(i, i+4) and $d_{\alpha\beta}$(i, i+3), and coupling constants $^3J_{HNH\alpha}$, as well as the chemical shift index of the α-protons are also summarized in Figure 2.

Coupling Constants

Twenty-four (24) $^3J_{HNH\alpha}$ coupling constants were measured by the well-dispersed ^{1}H and the DQF-COSY spectrum. Nine (9) of the 24 coupling constants were converted

into angle restraints, the others being in the range between 7–8 Hz.

Hydrogen Bonds

Amide protons, which are still visible after 12 hours exchanging, were considered as being engaged in hydrogen bonds (Fig. 2). The acceptors of hydrogen bonds for the slowly exchanged amide protons were identified during the structure refinement.

Secondary Structure

Secondary structural elements of BmKK2 were identified using the unique NOESY contacts, and $^3J_{HNH\alpha}$ coupling constants. A continuous set of strong d_{NN}(i, i+1) NOEs were observed in segment from Asp10 to Lys16, which is indicative of a helical conformation. The deduction was supported by a serial of medium-range NOEs of $d_{\alpha N}$(i, i+4), $d_{\alpha N}$(i, i+3) and $d_{\alpha\beta}$(i, i+3). Further corroborative data came from $^3J_{HNH\alpha}$ coupling constants and chemical shift index. Most of the $^3J_{HNH\alpha}$ coupling constants between residues 10-16 are smaller than 6.0 Hz. The chemical shifts of the α-protons of the residues Asp10, Ala11, Asp12, Ser14 and Arg15 up-field shifted by more than 0.1 ppm (Fig. 2). These data further confirmed above assignment of the helical element.

In addition, strands Ile5-Lys6, Cys23-Arg24, and Phe27-Cys28 showed strong sequential $d_{\alpha N}$ connectivities, and the residues Cys23, Arg24 and Phe27 indicated large $^3J_{HNH\alpha}$ ($>$ 8.0 Hz) coupling constants. Meanwhile, a network of long-range $d_{\alpha N}$, $d_{\alpha\alpha}$ and d_{NN} NOEs were observed for the strands of Ile5-Lys6, Cys23-Arg24 and Phe27-Cys28, such as $d_{\alpha\alpha}$(Lys6, Phe27), $d_{\alpha N}$ (Lys6, Cys28), $d_{\alpha N}$ (Phe27, Cys7) and d_{NN} (Arg24, Phe27). These observations suggested the presence of a three-stranded β-sheet. The location of the β sheet element was also confirmed by the slowly exchanging amide proton data. As shown in Figure 2 all the amide protons involved in the central strand were slowly exchanged, whereas the amide protons of the residue Arg24 involved in one external strand also exhibited slow exchange. The hydrogen bond partner of amide proton of Cys7 and Cys28 were identified as the carbonyl oxygen of Gly26 and Ile5, respectively during the structure calculation. The strands Cys23-Arg24 and Phe27-Cys28 were connected by a type I' β-turn comprised of residues 24–27.

Structure Calculation and Refinement

The input for distance geometry calculations with the program DYANA consisted of upper distance limits obtained from NOESY (mixing time 200 ms) cross-peak intensities with the program CALIBA,[46,47] and dihedral angle constraints derived from an initial interpretation of the vicinal coupling constants $^3J_{HNH\alpha}$. For the calibration of proton-proton distance limits (r versus the cross-peak intensities), the dependence of $1/r^6$ was used for all protons. These calibration curves were refined based on the plotting cross peak volume versus average proton–proton distance according to the preliminary structures. A total of 249 distance constraints were used, which can be clustered into 144 intra-residual, 69 sequential, 14 medium-range ($1 < |i - j| \leq 4$), 22 long-range ($|i - j| > 4$) NOE's. Nine ϕ angle constraints ($-55 \pm 15°$ for $^3J_{HNH\alpha} < 6.0$ Hz, $-120 \pm 35°$ for $^3J_{HNH\alpha} > 9.0$ Hz and $-120 \pm 45°$ for 9.0 Hz $> {}^3J_{HNH\alpha} > 8.0$ Hz) were used for structure calculation. In addition, nine distance constraints were added for three disulfide bonds (three per bond). Five slow-exchanging amide protons were determined from the H-D exchanging TOCSY spectra. Hydrogen bond constraints were imposed between slow-exchanging amide protons and their receptors based on the DYANA preliminary structures. For each hydrogen bond, two limit restraints were used between the NH-O (0.22 nm) and the N-O (0.32 nm) atom pairs. In addition, five stereo-specific assignments of methylene protons were obtained on the basis of the preliminary structures by the program GLOMSA.[46,47] Totally, 282 constraints (average 9.1 constraints per residue) were obtained and used in the structure calculations of BmKK2.

The structures were calculated using the program DYANA[35] on a SGI Indigo II computer. Starting from 200 random structures, 35 preliminary structures with lowest target functions obtained from distance geometry calculations were subjected to restrained energy minimization (REM) using the SANDER module of the AMBER 5.0 package.[36,37] A cutoff radius of 0.8 nm for non-bonded interactions, with a residue-based pair-list routine, was used in all calculations. Energy minimization was performed using a combination of steepest descent and conjugate gradient algorithms with a gradient convergence norm of less than 10^{-4} kJ mol^{-1} nm^{-1}. After energy minimization with AMBER, the 15 best DYANA conformers with the lowest energy were used to represent the solution conformation of BmKK2.

Solution Structure of BmKK2

Figure 3(a) represents the superimposition of the polypeptide backbones of 15 best conformers. No NOE violations larger than 0.10 Å and no angle violations larger than 5° were found. The overall agreement among individual conformers was indicated by global root-mean-square deviation (RMSD). The final set of 15 structures displayed an overall RMSD of 1.67 Å for the backbone atoms and 2.50 Å for all heavy atoms. However, the RMSD values for backbone atoms and the heavy atoms were changed to 0.69 Å and 1.61 Å, respectively, if the first three residues and the last residue of the toxin were not taken into consideration. Analysis of the ensemble of 15 structures using PROCHECK_NMR revealed that 65.8% of residues lie in most favored regions, 27.8% of residues in additionally allowed regions, and 6.1% of residues in generously allowed regions of the Ramachandran ϕ,ψ dihedral angle plot (plot not shown).

The structure of BmKK2 with the lowest energy is shown in Figure 3(b). The molecule adopts the α/β-fold motif, which consists of a three-stranded anti-parallel β-sheet anchored to a single α-helix (Asp10-Lys16) by three disulfide bridges (Cys7-Cys23, Cys13-Cys28 and Cys17-Cys30). The β-sheet involves residues Ile5-Lys6 (strand I), Cys23-Arg24 (strand II) and Phe27-Cys28

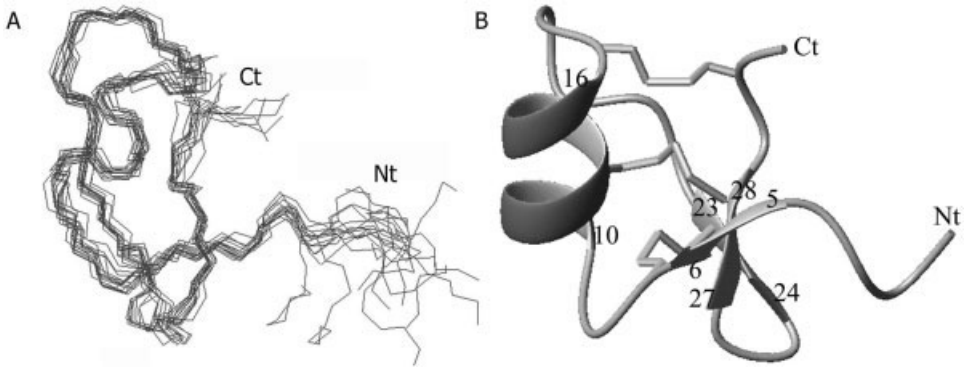

Fig. 3. **A**: Backbone superimposition of the best 15 structures of BmKK2. Nt and Ct indicate N-terminus and C-terminus, respectively. **B**: MOLMOL representation of the structure of BmKK2 with the lowest energy. Secondary structural elements are drawn with three disulfide bridges (neons). Beginning and ending residues of each secondary structure element are labeled according to protein sequence. Nt and Ct indicate N-terminus and C-terminus, respectively.

(strand III) which are connected by a type I′ β-turn (residues 24–27).

Structural Features of BmKK2

Despite BmKK2 adopting a common α/β-motif, it showed distinct local conformation from other typical K^+ toxin (e.g., CTX and NTX) especially in the loop structure between α-helix and β-sheet, as well as in the N-terminal and C-terminal regions. The backbone of the residues involved in these three parts of BmKK2 matched poorly with the corresponding residues of CTX and NTX, as shown in Figure 4. In addition, the helix is shorter and the three-stranded β-sheet is smaller (each strand consisted of only two residues), while its N-terminus and C-terminus were extended in BmKK2.

The sequence alignments of BmKK2 and other similar short-chain K^+-toxins are shown in Figure 5. Compared with other K^+-toxins like CTX, the most distinct feature of the primary sequence in BmKK2 is the shorter peptide segment (Pro18-Pro22) between the third and fourth Cys residue, which only contains five residues and three of them are Pro residues. Consecutive two Pro residues at position 21 and 22 of BmKK2 are very unusual. It was well known that Pro residue is the interrupter of regular secondary structure of protein due to lack of amide proton, which usually can be used as the donor in forming a hydrogen bond to stabilize the secondary structure. The residue Pro22 of BmKK2 disrupted the hydrogen bond network of the anti-parallel β-sheet of this toxin and further resulted in the interruption of β-strands. The destroying of the β-sheet structure of BmKK2 was aggravated by the effect from the residue Pro21 of this toxin. Usually, these two positions are highly conserved in short-chain scorpion K^+-toxins known, and most scorpion toxins contain a Gly and a Lys residue at the corresponding positions (Fig. 5). The shortening of the central strand in the β-sheet structure of BmKK2 could be well explained by the displacement of the residue Gly and Lys by Pro at position 21 and 22 of this toxin. It was suggested by Bontems et alobic contacts also contributed to the stable

```
          1                                                  40
BmKK2   -TPFAIKCATDADCSRKCPGN------PPCRNGFCACT--
 CTX    -ZFTNVSCTTSKECWSVCQRLHNTSR-GKCMNKKCRCYS-
 KTX    GVEINVKCSGSPQCLKPCKDA-GMRF-GKCMNRKCHCTPK
 MTX    -----VSCTGSKDCYAPCRKQTGCPN-AKCINKSCKCYGC*
 NTX    -TIINVKCTSPKQCSKPCKELYGSSAGAKCMNGKCKCYNN
 P01    -----VSC---EDCPEHCSTQ-KAQ—AKCDNDKCVCEPI
 ScTX   -----AFC-NLRMCQLSCRSL-GLL—GKCIGDKCECVKH
 TSK    -VVIGQRCYRSPDCYSACKKLVGKAT-GKCTNGRCDC---
 CoTX1  -----AVC-VYRTCDKDCKRR-GYRS-GKCINNACKCYPY
```

Fig. 5. Sequences alignment of BmKK2 with those of other similar short-chain scorpion K^+-toxins. The amino acid sequences are aligned according to their cysteine residues and the cysteines are boxed. An asterisk indicates amidation at the C terminus. Gaps are presented as dashes. CTX, charybdotoxin from *Leiurus quinquestriatus hebraeus*. KTX, kaliotoxin from *Androctonus mauretanicus mauretanicus*. MTX, maurotoxin from *Scorpio maurus*. NTX, noxiustoxin from *Centruroides noxius*. P01 from *Androctonus mauretanicus mauretanicus*. ScTX, scyllatoxin from *Leiurus quinquestriatus hebraeus*. TSK, TsKapa from *Buthidae Tityus serrulatus*. CoTX1, cobatoxin from *Centruroides noxius*.

binding of the toxin and[48] that Cys-[…]-Cys-x-x-x-Cys-[…]-**Gly**-x-Cys-[…]-Cys-x-Cys was the signature sequence for scorpion toxins to form α/β folds and the Gly in this sequence was conserved due to steric hindrance between the helix and the sheet. Later studies found that the replacement of this Gly with an Ala did not disturb the global folding significantly, as in NTX, MTX, and P01. It appeared that the methyl side chain of the alanine could be accommodated when the helix was bent slightly.[49] In BmKK2, the non β-sheet conformation of the residue Pro21 and Pro22 made it become acceptable by the moving of its the bulky side chain away from the hydrophobic core structure. This kind of arrangement of side chains minimized the overlapped surface with α-helix, where two basic residues (Arg15 and Lys16) are located, and reduced the energy cost of such an overlap. Therefore, BmKK2 possessed a smaller and most condensed core structure in comparison with those of other short-chain scorpion tox-

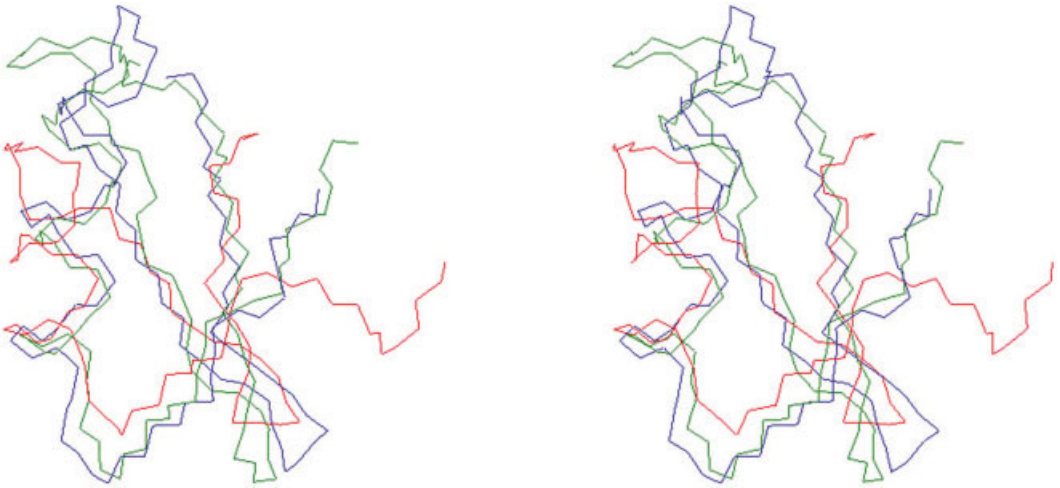

Fig. 4. Stereoview of the backbone superposition of BmKK2 (in red) with CTX (in blue) and NTX (in dark green). CTX and NTX coordinates were obtained from the Protein Data Bank with accession Nos. 2CRD and 1SXM, respectively.

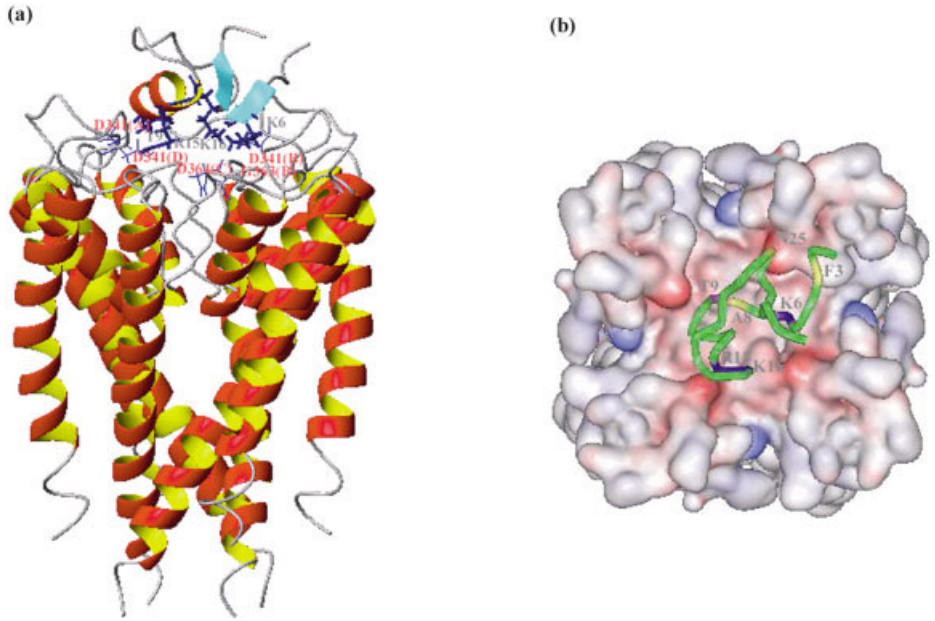

Fig. 6. The complex of BmKK2 and the rSK2 channel. **a**: The two molecules are represented as ribbon structures. The closest contacts Lys6 -Asp341 (B), Lys6-Gly363 (B), Thr9-Asp341 (A), Arg15-Asp341 (D), and Lys16 -Asp364(C). **b**: The top view of the complex shown in (a), generated from the program WebLab ViewerPro 4.0. The rSK2 channel is represented as a molecular surface colored by electrostatic potential and BmKK2 as a green tube structure. The positive residues Lys6, Arg15, and Lys16 are displayed in blue, while residues Phe3, Ala8 and Asn25 which participate in hydrophobic contacts are displayed in yellow.

ins, which predicted that a K^+ channel with a narrower entryway was likely be preferred for BmKK2 toxin.

Interaction of BmKK2 With rSK Channels

The specificity of scorpion toxins for the various potassium channels has been extensively investigated. The results revealed that binding of the peptides is governed by electrostatic interactions between negatively-charged residues in the channel and positively charged residues in the peptide. The surface electrostatic distribution analysis indicated that BmKK2 preferred association with the entryway of the rSK2 channel using its positive patch around the side chains of Lys 6, Arg 15, and Lys 16. The most favorable docked conformation was found with the closest contacts Lys6-Asp341 (B), Lys6-Gly363 (B), Thr9-Asp341 (A), Arg15-Asp341 (D), and Lys16-Asp364(C) between BmKK2 and K^+ channel. The structures of BmKK2/rSK2 channel clusters with the favorable electrostatic energy were further refined and the optimized structure of BmKK2-rSK2 channel complex is shown in Figure 6.

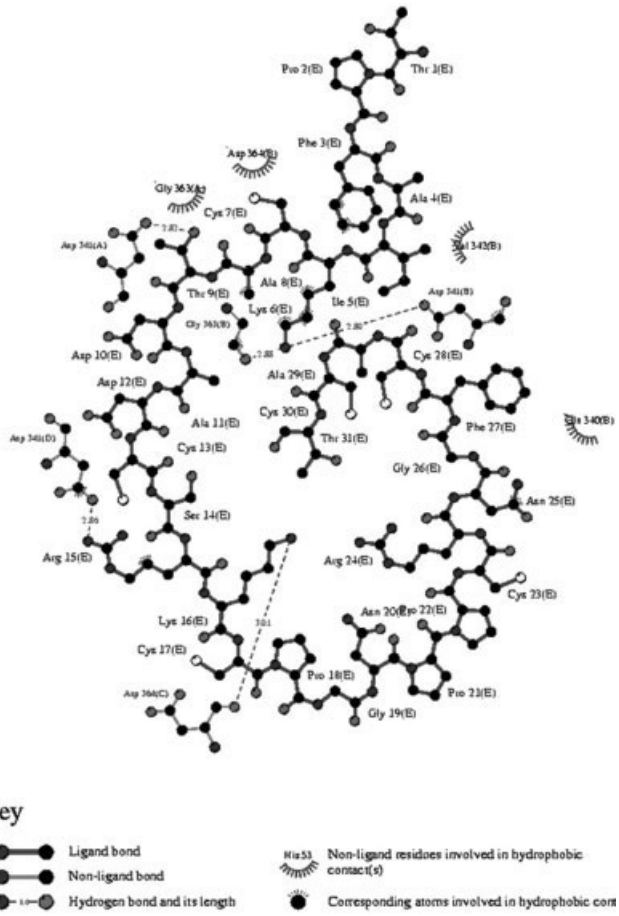

Fig. 7. A depiction (generated by LIGPLOT) of the main interactions between the scorpion toxin BmKK2 and the rSK2 channel.

TABLE I. The Hydrogen Bonds Between the BmKK2 Scorpion Toxin and the rSK2 Channel in the BmKK2-rSK2 Channel Complex

Scorpion toxin BmKK2		rSK2 channel		
Residue	Atom	Residue[a]	Atom	Distance (Å)
Lys6	NZ	Asp341 (B)	OD1	2.80
Lys6	NZ	Gly363 (B)	O	2.88
Thr9	OH	Asp341 (A)	OD1	2.82
Arg15	NH1	Asp341 (D)	OD2	2.86
Lys16	NZ	Asp364 (C)	O	3.01

[a]A,B,C and D represent the four chains of the rsk2 channel.

The principal BmKK2-rSK2 channel interactions derived from the refined structure were analyzed using the LIGPLOT program[50,51] and is displayed in Figure 7. As indicated in Figure 7, five hydrogen bonds existed in the refined complex (see Table I). Meanwhile, the favorable electrostatic interactions between the two proteins were found in the refined structure of the complex, including three positively-charged Arg residues of BmKK2 interacting with four negatively-charged Asp residues of rSK2 channel as shown in Figure 7.

TABLE II. The Hydrophobic Contacts Between the BmKK2 Scorpion Toxin and the rSK2 Channel in the BmKK2-rSK2 Channel Complex

Scorpion toxin BmKK2	rSK2 channel
Phe3	Asp341 (B)
Phe3	Val342 (B)
Lys6	Gly363 (B)
Lys6	Asp364 (B)
Ala8	Gly363 (A)
Arg15	Asp341 (D)
Asn25	Gln340 (B)

In addition to these five critical interaction pairs of residues, the hydrophobic contacts also contributed to the stable binding of the toxin and K^+ channel, which are summarized in Table II. Therefore, the interface between the BmKK2 and rSK2 channel is large and involves about seven residues of BmKK2 and nine residues of the K^+ channel, respectively.

Interaction of BmKK2 With Kv channels

The same analysis was applied on the contacts between BmKK2 and the hKv1.3 channel. BmKK2 was docked into the entryway of the hKv1.3 channel along with the dipole direction. The closest contacts found in the BmKK2/hKv1.3 channel complex included Lys6/Gly396 (B), Lys6/His399 (B), Arg15/Gly396 (D), Arg15/Asp397 (D), and Lys16/Asp397 (C). However, the side-chain of Phe3 could bump into the turret of the S5-S6 loop of hKv1.3. After energy minimization and dynamic simulation, the principal BmKK2-hKv1.3 channel interactions derived from the refined structure were analyzed and displayed using the LIGPLOT program (not shown here, available as supporting material). Clearly, weaker interactions were found in this complex model: only two hydrogen bonds formed, one from Lys6 (BmKK2) with Gly396 (B) (hKv1.3) and one from Lys16 (BmKK2) with Asp397 (C) (hKv1.3), as well as one hydrophobic contact between the side-chains of Lys6 (BmKK2) and Asp397 (B) (hKv1.3).

Structure-Function Relation

The structure-function relationship of scorpion toxins for the various potassium channels has been studied through the generation of mutants both in ion channels and toxins.[52–56] The results revealed that the binding site of scorpion toxins are composed of residues located in the outer vestibule near the pore of potassium channel. The scorpion toxins block the ion conduction through potassium channels by physically occluding the pore at the extra-cellular opening.[57] Binding of the peptides occurs through a reversible, bimolecular reaction, which is governed by electrostatic interactions between negatively charged residues in the channel and positively charged residues in the peptide. Mutational analysis of CTX showed that five residues Lys27, Met29, Asn30, Arg34, and Tyr36, located in the β-sheet and the β-turn, are important for the binding of CTX to a voltage-dependent K^+ channel (*Shaker* B).[52–54, 58] Among these residues, Lys27 is the most

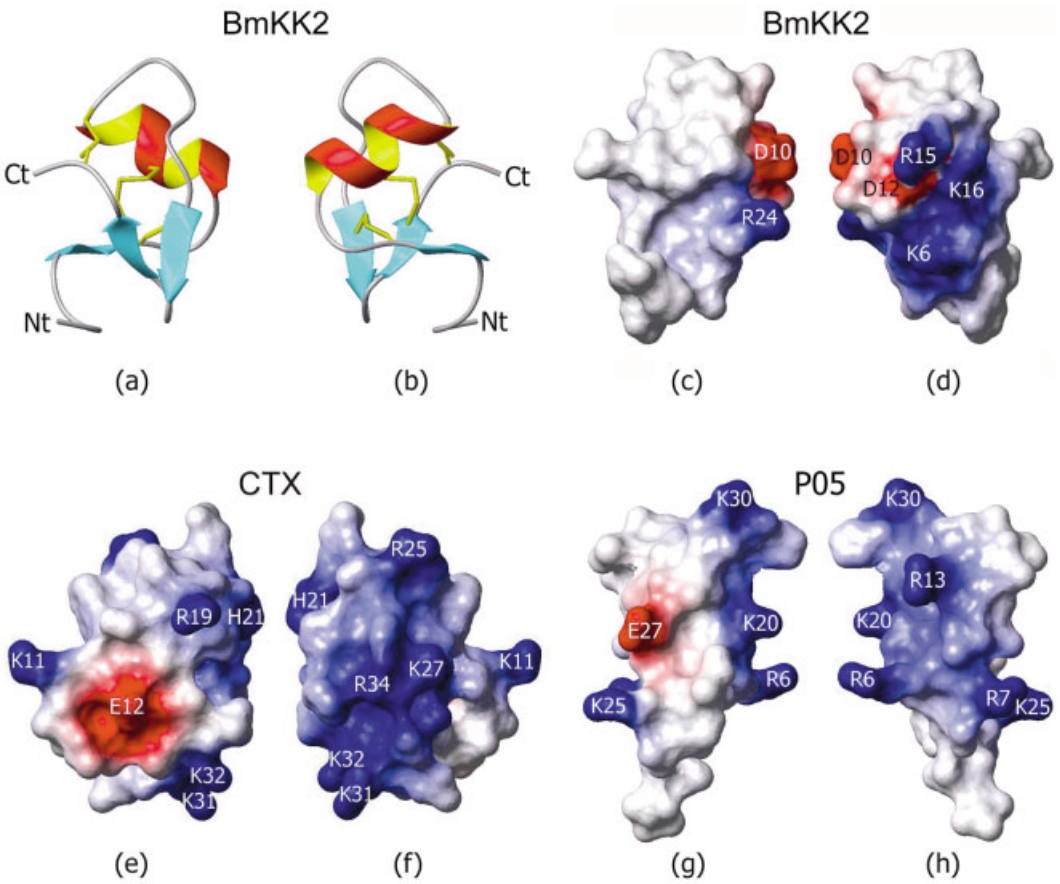

Fig. 8. Structure and electrostatic potentials of the water accessible surfaces of three α-KTx toxins. **a, b**: MOLMOL representation of the structure of BmKK2 with the lowest energy. Nt and Ct indicate N-terminus and C-terminus, respectively. **c–h**: Simple charge electrostatic potentials associated to the water-accessible molecular surfaces of α-KTx toxins calculated using MOLMOL. Positively-charged residues and negatively-charged residues are shown in blue and in red, respectively. Molecules in c, f, and g are in the same orientation of a, and molecules in d, e, and h are in the same orientation of b.

important one and it is suspected to directly plug into the pore, coming in the vicinity of the selectivity filter of potassium channel.[57] The characteristics of five corresponding residues of NTX are similar to those in CTX, and thus NTX also exhibits high affinity for Kv channel.[16]

As demonstrated previously, the 3D solution structures of scorpion toxins possess a classic motif with an antiparallel β-sheet face on one side of the molecule and a helix on the other. The interaction mode and molecular recognition of various peptide toxins and several K^+ channels have been studied by docking calculation and dynamic simulation.[44,59] As a typical interaction mode of scorpion toxins and K^+ channels, the tight binding between the solvent-exposed surface of β-sheet of the toxin and potassium Kv channel was found for CTX and Agitoxin2, which may be referred to β-type binding.

On the other hand, a different interaction mode has been reported for the scorpion toxin P05 and rSK channel, in which the α-helix element of P05 toxin associates with the entryway of SK channel. The critical residues of P05 for binding to rSK2 channel are three basic residues: Arg6, Arg7, and Arg13. These three Arg residues are all located in the α-helix of P05 with the greatest positive potential. The interface of BmKK2 with rSK2 channel mainly covers the surface of the α-helix side of the molecule. Thus, their interaction mode may refer as α-type binding.

For comparison, the surface electrostatic charge distribution of BmKK2, P05, and CTX peptides are shown in Figure 8. As shown in the Figure 8, BmKK2 contains a dense positively-charged region composed mainly by Lys6, Arg15, and Lys16 at the N terminus. Lys6 is located at the terminal of first sheet and its side-chain is pointed to the helix direction, while Arg15 and Lys16 are located at the end of the α-helix. It is clear that the interaction mode of BmKK2 towards K^+ channel should be similar with that (α-type) of P05, but is distinct from those (β-type) of CTX and NTX toxin.

Compared with CTX and NTX, which displayed strong binding affinity for Kv channels,[60,16] BmKK2 exhibited only weaker inhibitory activity towards the voltage-gated K^+ channels (the IC_{50} values at μM level). In order to clarify the possible reason, two models of BmKK2/hKv1.3 channel and BmKK2/rSK2 channel complexes have been studied by docking and simulation in the present study. The model of BmKK2 and rSK channel complex with a narrow entryway showed more favorable contacts both in

electrostatic and hydrophobic. It possessed five hydrogen bonds and a bigger interface containing seven pairs of inter-residue interactions. On the other hand, the model of BmKK2 and Kv channel complex demonstrated poor contacts, a smaller interface, and less inter-residue interactions (three pairs). These results well explained its lower activity towards Kv channels and also suggested that it may prefer a SK-type-like channel with narrower entryway as its specific receptor. To validate these predictions additional functional investigations will be necessary.

Data Bank Accession Numbers

The chemical shifts of BmKK2 at pH3.0 and 300 K have been deposited to BioMagResBank (BMRB) under accession No. 5865. The atomic coordinates of the 15 energy-minimized conformers used to represent the solution structure of BmKK2 have been deposited in the Brookhaven data bank, together with the input of conformational restrains used for the structure calculation under accession No. 1PVZ.

ACKNOWLEDGEMENTS

The authors thank the Institute of Molecular biology and Biophysics, ETH-Hönggerberg Zürich, Switzerland, for giving the programs DYANA (version 1.5) and XEASY. We also thank Prof. Bertini of Florence University, Italy, for the the program CALIBA and Prof. James W. Caldwell of California University, U.S.A., for program AMBER, as well as Tripos, Inc., for the Sybyl6.3 software package.

REFERENCES

1. Rochat H, Bernard P, Couraud F. Scorpion toxins: chemistry and mode of action. In: Ceccarelli B, Clementi F, editor. Advances in cytopharmacology. Vol 3B. New York: Raven Press; 1979. p 325–334.
2. Possani LD. In: Tu AT, editor. Handbook of natural toxins. Vol 2. New York: Marcel Dekker Inc.; 1984. p 513–550.
3. Zlotkin E, Eitan M, Bindokas VP, Adams ME, Moyer M, Burkhart W, Fowler E. Functional duality and structural uniqueness of depressant insect-selective neurotoxins. Biochemistry 1991;30: 4814–4821.
4. Kopeyan C, Martinez G, Lissitzky S, Miranda F, Rochat H. Disulfide bonds of toxin II of the scorpion *Androctonus australis* Hector. Eur J Biochem 1974;47:483–489.
5. Carbone E, Wanke E, Prestipino G, Possani LD, Maelicke A. Selective blockage of voltage-dependent K^+ channels by a novel scorpion toxin. Nature 1982;296:90–91.
6. Martin BM, Ramirez AN, Gurrola GB, Nobile M, Prestipino G, Possani LD. Novel K(+) channel-blocking toxins from the venom of the scorpion Centruroides limpidus limpidus Karsch. Biochem J 1994;304(Pt1):51–56.
7. Rogowski RS, Collins JH, O'Neill TJ, Gustafson TA, Werkman TR, Rogawski MA, Tenenholz TC, Weber DJ, Blaustein MP. Three new toxins from the scorpion Pandinus imperator selectively block certain voltage-gated K^+ channels. Mol Pharmacol 1996;50:1167–1177.
8. Olamendi-Portugal T, Gomez-Lagunas F, Gurrola GB, Possani LD. A novel structural class of K^+ channel blocking toxin from the scorpion Pandinus imperator. Biochem J 1996;315:977–981.
9. Garcia ML, Gao Y-D, McManus OB, Kaczorowski GJ. Potassium channels: from scorpion venoms to high-resolution structure. Toxicon 2001;39:739–748.
10. Garcia-Calvo M, Knaus HG, McManus OB, Giangiacomo KM, Kaczorowski GJ, Garcia ML. Purification and reconstitution of the high-conductance, calcium-activated potassium channel from tracheal smooth muscle. J Biol Chem 1994;269:676–682.
11. Garcia ML, Hanner M, Knaus HG, Koch R, Schmalhofer W, Slaughter RS, Kaczorowski GJ. Pharmacology of potassium channels. Adv Pharmacol 1997;39:425–471.
12. Possani LD, Martin BM, Svenden IB. The primary structure of noxiustoxin: A K^+ channel blocking peptide purified from the venom of the scorpion Centruroides noxius Hoffmann. Carlsberg Res Commun 1982;47:285–289.
13. Tytgat J, Chandy KG, Garcia ML, Gutman GA, Martin-Eauclaire MF, et al. A unified nomenclature for short-chain peptides isolated from scorpion venoms: alpha-KTx molecular subfamilies. Trends Pharmacol Sci 1999;20:444–447.
14. Goudet C, Chi C-W, Tytgat J. An overview of toxins and genes from the venom of the Asian scorpion *Buthus martensi* Karsch. Toxicon 2002;40:1239–1258.
15. Bontems F, Roumestand C, Boyot P, Gilquin B, Doljansky Y, Menez A, Toma F Three-dimensional structure of natural charybdotoxin in aqueous solution by 1H-NMR. Charybdotoxin possesses a structural motif found in other scorpion toxins. Eur J Biochem 1991;196:19–28.
16. Dauplais M, Gilquin B, Possani LD, Gurrola-Briones G, Roumestand C, Menez A. Determination of the three-dimensional solution structure of noxiustoxin: analysis of structural differences with related short-chain scorpion toxins. Biochemistry 1995;34:16563–16573.
17. Blanc E, Romi-Lebrun R, Bornet O, Nakajima T, Darbon H. Solution structure of two new toxins from the venom of the Chinese scorpion *Buthus martensi* Karsch blockers of potassium channels. Biochemistry 1998;37:12412–12418.
18. Meunier S, Bernassau JM, Sabatier JM, Martin-Eauclaire MF, Van Rietschoten J, Cambillau C, Darbon H. Solution structure of P05-NH2, a scorpion toxin analog with high affinity for the apamin-sensitive potassium channel. Biochemistry 1993;32: 11969–11976.
19. Fernandez I, Romi R, Szendeffy S, Martin-Eauclaire MF, Rochat H, Van Rietschoten J, Pons M, Giralt E. Kaliotoxin (1-37) shows structural differences with related potassium channel blockers. Biochemistry 1994;33:14256–14263.
20. Wang I, Wu S-H, Chang H-K, Shieh R-C, Yu H-M, Chen C. Solution structure of a K(+)-channel blocker from the scorpion Tityus cambridgei. Protein Sci 2002;11:390–400.
21. Wu G, Li Y, Wei D, He F, Jiang S, Hu G, Wu H. Solution structure of BmP01 from the venom of scorpion *Buthus martensii* Karsch. Biochem Biophys Res Commun 2000;276:1148–1154.
22. Wu G, Wei DS, He FH, Hu GY, Wu HM. A K^+ channel-blocking peptide from venom of Chinese scorpion *Buthus martensii* Karsch. Acta Pharmacologica Sinica 1998;19:317–321.
23. Zeng XC, Peng F, Luo F, Zhu SY, Liu H, Li WX. Molecular cloning and characterization of four scorpion K(+)-toxin-like peptides: a new subfamily of venom peptides (alpha-KTx14) and genomic analysis of a member. Biochimie 2001;83:883–889.
24. Zhang J-M, Hu G-Y. Huperzine A, a nootropic alkaloid, inhibits N-methyl-D-aspartate-induced current in rat dissociated hippocampal neurons. Neuroscience 2001;105:663–669.
25. Klee R, Ficker E, Heinemann U. Comparison of voltage-dependent potassium currents in rat pyramidal neurons acutely isolated from hippocampal regions CA1 and CA3. J Neurophysiol 1995;74: 1982–1995.
26. Wu HM, Wu G, Huang XL, He FH, Jiang SK. Purification, characterization and structural study of the neuro-peptides from scorpion *Buthus martensi* Karsch. Pure Appl Chem 1999;71:1157–1162.
27. Piantini U, Sorensen OW, Ernst RR. Multiple quantum filters for elucidating NMR coupling networks. J Am Chem Soc 1982;104: 6800–6801.
28. Braunschweilier L, Ernst RR. Coherence transfer by isotropic mixing: application to proton correlation spectroscopy. J Magn Reson 1988;53:521–528.
29. Griesinger C, Otting G, Wüthrich K, Ernst RR. Clean TOCSY for proton spin system identification in macromolecules. J Am Chem Soc 1988;110:7870–7872.
30. Jeener J, Meier BH, Bachmann P, Ernst RR. Investigation of exchange process by two-dimensional NMR spectroscopy. J Chem Phys 1979;71:4546–4553.
31. Drobny G, Pines A, Sinton S, Weitekamp D, Wemmer,D. Fourier transform multiple quantum nuclear magnetic resonance. Faraday Symp Chem Soc 1979;13:49–55.
32. Bax AD, Davis DG. MLEV-17-based two-dimensional homo-

nuclear magnetization transfer spectroscopy. J Magn Reson 1985; 65:355–366.
33. Bartels C, Xia T-H, Billeter M, Güntert P, Wüthrich K. The program XEASY for computer-supported NMR spectral analysis of biological macromolecules. J Biomol NMR 1995;6:1–10.
34. Wüthrich K. NMR of proteins and nucleic acid. New York: John Wiley & Sons; 1986. 292 p.
35. Güntert P, Mumenthaler C, Wüthrich K. Torsion angle dynamics for NMR structure calculation with the new program DYANA. J Mol Biol 1997;273:283–298.
36. Weiner SJ, Kollman PA. AMBER: assisted model building with energy refinement. A general program for modeling molecules and their interactions. J Comput Chem 1981;2:287–309.
37. Weiner SJ, Kollman PA, Nguyen DT, Case DA. An all-atom force field for simulations of proteins and nucleic acids. J Comput Chem 1986;2:230–252.
38. Laskowski RA, MacArthur MW, Moss DS, Thornton JM. PROCHECK: a program to check the stereochemical quality of protein structures. J Appl Crystallogr 1993;26:283–291.
39. Laskowski RA, Rullmann JAC, MacArthur MW, Kaptein R, Thornton JM. AQUA and PROCHECK-NMR: programs for checking the quality of protein structures solved by NMR. J Biomol NMR 1996;8:477–486.
40. Koradi R, Billeter M, Wüthrich K. MOLMOL: a program for display and analysis of macromolecular structures. J Mol Graph 1996;14:51–55.
41. Folander K, Douglass J, Swanson R. Confirmation of the assignment of the gene encoding Kv1.3, a voltage-gated potassium channel (KCNA3) to the proximal short arm of human chromosome 1. Genomics 1994;23:295–296.
42. Köhler M, Hirschberg B, Bond CT, Kinzie JM, Marrion NV, Maylie J, Adelman JP. Small-conductance, calcium-activated potassium channels from mammalian brain. Science 1996;273: 1709–1714.
43. Doyle DA, Morais Cabral J, Pfuetzner RA, Kuo A, Gulbis JM, Cohen SL, Chait BT, Mackinnon R. The structure of the potassium channel: molecular basis of K^+ conduction and selectivity. Science 1998;280:69–77.
44. Gao Y-D, Maria LG. Interaction of agitoxin2, charybdotoxin, and iberiotoxin with potassium channels: selectivity between voltage-gate and maxi-K channels Proteins 2003;52:146–154.
45. Jones TA, Kjeldgaard M. "Essential O" software manual. Uppsala University, Uppsala, Sweden; 1998.
46. Güntert P, Braun W, Wüthrich K. Efficient computation of three-dimensional protein structures in solution fromnuclear magnetic resonance data using the program DIANA and the supporting programs CALIBA, HABAS and GLOMSA. J Mol Biol 1991;217:517–530.
47. Güntert P, Qian YQ, Otting G, Muller M, Gehring WJ, Wüthrich K. Structure determination of the Antp (C39—S) homeodomain from nuclearmagnetic resonance data in solution using a novel strategy for the structure calculation with the programs DIANA, CALIBA, HABAS and GLOMSA. J Mol Biol 1991;217:531–540.
48. Bontems F, Roumestand C, Gilquin B, Toma F. Refined structure of charybdotoxin: common motifs in scorpion toxins and insect defensins. Science 1991;254:1521–1523.
49. Blanc E, Sabatier JM, Kharrat R, Meunier S, el Ayeb M, Van Rietschoten J, Darbon H. Solution structure of maurotoxin, a scorpion toxin from Scorpio maurus, with high affinity for voltage-gated potassium channels. Proteins 1997;29:321–33.
50. McDonald IK, Thornton JM. Satisfying hydrogen bonding potential in proteins. J Mol Biol 1994;238:777–793.
51. Wallace AC, Laskowski RA, Thornton JM. LIGPLOT: a program to generate schematic diagrams of protein-ligand interactions. Protein Eng 1995;8:127–134.
52. Stampe P, Kolmakova-Partensky L, Miller C. Intimations of K^+ channel structure from a complete functional map of the molecular surface of charybdotoxin. Biochemistry 1994;33:443–450.
53. Goldstein SAN, Pheasant DJ, Miller C. The charybdotoxin receptor of a Shaker K+ channel: peptide and channel residues mediating molecular recognition. Neuron 1994;12:1377–1388.
54. Naranjo D, Miller C. A strongly interacting pair of residues on the contact surface of charybdotoxin and a Shaker K^+ channel. Neuron 1996;16:123–130.
55. Park CS, Miller C. Interaction of charybdotoxin with permeant ions inside the pore of a K^+ channel. Neuron 1992;9:307–313.
56. Pardo-Lopez L, Zhang M, Liu J, Jiang M, Possani LD, Tseng G-N. Mapping the binding site of a human ether-a-go-go-related gene-specific peptide toxin (ErgTx) to the channel's outer vestibule. J Biol Chem 2002;277:16403–16411.
57. Aiyar J, Rizzi JP, Gutman GA, Chandy KG. The signature sequence of voltage-gated potassium channels projects into the external vestibule. J Biol Chem 1996;271:31013–31016.
58. Gross A, MacKinnon R. Agitoxin footprinting the shaker potassium channel pore. Neuron 1996;16:399–406.
59. Cui M, Shen J-H, James MB, Fu W, Wu J-J, Zhang Y-M, Luo X-M, Chi Z-W, Ji R-Y, Jiang H-L, Chen K-X. J Mol Biol 2002;318:417–428.
60. Aiyar J, Withka JM, Rizzi JP, Singleton DH, Andrews GC, Lin W, Boyd J, Hanson DC, Simon M, Dethlefs B, et al. Topology of the pore-region of a K^+ channel revealed by the NMR-derived structures of scorpion toxins. Neuron 1995;15:1169–1181.